Ovchinnikov, Yu. A., Gubanov, V. V., Khramtsov, N. V., Ischenko, K. A., Zagranichny, V. E., Muradov, K. G., Shuvaeva, T. M., & Lipkin, V. M. (1987) *FEBS Lett.* *223*, 169–173.

Puskas, R., Fredd, N., Gazdar, C., & Peterkofsky, A. (1983) *Arch. Biochem. Biophys.* *223*, 503–513.

Stryer, L. (1986) *Annu. Rev. Neurosci.* *9*, 87–119.

Tomita, T. (1970) *Q. Rev. Biophys.* *3*, 179–222.

Tuteja, N., & Farber, D. B. (1988) *FEBS Lett.* *232*, 182–186.

Vieira, J., & Messing, J. (1987) *Methods Enzymol.* *153*, 3–11.

Wensel, T. G., & Stryer, L. (1986) *Proteins 1*, 90–99.

Woodruff, M. L., & Bownds, M. D. (1979) *J. Gen. Physiol.* *73*, 629–653.

Yamazaki, A., Stein, P. J., Chernoff, N., & Bitensky, M. W. (1983) *J. Biol. Chem.* *258*, 8188–8194.

Yau, K.-W., & Nakatani, K. (1985) *Nature 313*, 579–582.

Yee, R., & Liebman, P. A. (1978) *J. Biol. Chem.* *253*, 8902–8909.

Overcoming the Overlap Problem in the Assignment of ^{1}H NMR Spectra of Larger Proteins by Use of Three-Dimensional Heteronuclear ^{1}H–^{15}N Hartmann–Hahn–Multiple Quantum Coherence and Nuclear Overhauser–Multiple Quantum Coherence Spectroscopy: Application to Interleukin 1β[†]

Dominique Marion,[‡,§] Paul C. Driscoll,[‡] Lewis E. Kay,[‡] Paul T. Wingfield,[‖] Ad Bax,[‡] Angela M. Gronenborn,[*,‡] and G. Marius Clore[*,‡]

Laboratory of Chemical Physics, National Institute of Diabetes, Digestive and Kidney Diseases, National Institutes of Health, Bethesda, Maryland 20892, and Glaxo Institute for Molecular Biology SA, 46 Route des Acacias, CH-1227 Geneva, Switzerland

ABSTRACT: The application of three-dimensional (3D) heteronuclear NMR spectroscopy to the sequential assignment of the ^{1}H NMR spectra of larger proteins is presented, using uniformly labeled (~95%) [^{15}N]interleukin 1β, a protein of 153 residues and molecular mass of 17.4 kDa, as an example. The two-dimensional (2D) 600-MHz spectra of interleukin 1β are too complex for complete analysis, owing to extensive cross-peak overlap and chemical shift degeneracy. We show that the combined use of 3D ^{1}H–^{15}N Hartmann–Hahn–multiple quantum coherence (HOHAHA–HMQC) and nuclear Overhauser–multiple quantum coherence (NOESY–HMQC) spectroscopy, designed to provide the necessary through-bond and through-space correlations for sequential assignment, provides a practical general-purpose method for resolving ambiguities which severely limit the analysis of conventional 2D NMR spectra. The absence of overlapping cross-peaks in these 3D spectra allows the unambiguous identification of $C^\alpha H(i)$–$NH(i+1)$ and $NH(i)$–$NH(i+1)$ through-space nuclear Overhauser connectivities necessary for connecting a particular $C^\alpha H(i)$–$NH(i)$ through-bond correlation with its associated through-space sequential cross-peak. The problem of amide NH chemical shift degeneracy in the ^{1}H NMR spectrum is therefore effectively removed, and the assignment procedure simply involves inspecting a series of 2D ^{1}H–^{1}H slices edited by the chemical shift of the directly bonded ^{15}N atom. Connections between residues can be identified almost without any knowledge of the spin system types involved, though this type of information is clearly required for the eventual placement of the connected residues within the primary sequence. Strategies for obtaining identification of spin system types include traditional analysis of the spectrum of nonlabile protons, site-directed mutagenesis, and specific labeling of selected amino acids. It is envisaged that the intrinsic simplicity of the 3D heteronuclear spectra, even for proteins of 150–200 residues, will permit the development of efficient computer-assisted or automated sequential assignment methods.

The extension of nuclear magnetic resonance (NMR)[1] experiments from one to two dimensions [see Ernst et al. (1987) for a review] has played a key role in the development of methods for the determination of three-dimensional structures of macromolecules in solution. The first step of such structure determinations is the sequential assignment of the ^{1}H NMR spectrum by means of experiments that identify through-bond and sequential through-space connectivities. By spreading the resonances into two frequency dimensions, the concomitant increase in both resolution and information content enables these connectivities to be readily analyzed. To date, the spectra of a substantial number of small proteins (<100 residues) have

---

[1] Abbreviations: NMR, nuclear magnetic resonance; NOE, nuclear Overhauser effect; NOESY, nuclear Overhauser enhancement spectroscopy; HOHAHA, homonuclear Hartmann–Hahn spectroscopy; HMQC, heteronuclear multiple quantum coherence spectroscopy.

been completely assigned, and in some cases their three-dimensional structures have been determined [see Wüthrich et al. (1986, 1989), Clore and Gronenborn (1987, 1989), and Bax (1989) for reviews].

Despite these tremendous advances, the limitations in the application of purely 2D homonuclear experiments to larger proteins containing more than about 100 residues become rapidly apparent. First, the increase in the number of resonances leads to severe crowding and chemical shift degeneracy in the two-dimensional spectra, resulting in unresolvable ambiguities in the identification of both sequential and long-range NOEs. Second, the accompanying increase in the rotational correlation time leads to short T_2 and $T_{1\rho}$ relaxation times and to an increase in line widths. As all scalar correlation experiments (e.g., COSY, multiple quantum, and HOHAHA) are limited to cases where the line widths are not significantly greater than the size of the J couplings, the identification of complete amino acid proton spin systems becomes increasingly difficult as the size of the molecule increases.

In the last few years a number of experiments involving isotope labeling have been proposed to partially resolve these problems. Thus, for example, proton line widths can to some extent be reduced by the random incorporation of deuterium at about the 80% level (LeMaster, 1987; LeMaster & Richards, 1988; Torchia et al., 1988a). An alternative procedure which also results in spectral simplification makes use of ^{1}H-detected heteronuclear multiple quantum correlation (HMQC) experiments to establish one-bond correlations between protons and a directly bonded ^{15}N or ^{13}C atom (Mueller, 1979; Bax et al., 1983; Redfield, 1983; Markley et al., 1984; Roy et al., 1984; Sklenar & Bax, 1987a; Glushka & Cowburn, 1987), combined with isotope-edited NOESY experiments (Wilde et al., 1986; Griffey & Redfield, 1987; Rance et al., 1987; Bax & Weiss, 1987; Senn et al., 1987; Fesik et al., 1987). These experiments rely on the fact that the ^{1}H–^{15}N and ^{1}H–^{13}C couplings are large (90 and 125–160 Hz, respectively) and have met with considerable success in the case of both T4 lysozyme (McIntosh et al., 1987a,b) and staphylococcal nuclease (Torchia et al., 1988b, 1989). Unfortunately, specific labeling is both expensive and technically difficult as it may require the use of auxotrophic strains and further necessitates numerous sample preparations as well as the recording of a very large number of spectra. For this reason, efforts have been made to develop more general-purpose strategies.

One such approach involves completely labeling the protein with ^{15}N and recording 2D relayed ^{15}N–^{1}H HMQC–COSY, HMQC–HOHAHA, and HMQC–NOESY spectra (Gronenborn et al., 1989a,b; Shon & Opella, 1989). In this manner, ^{1}H–^{1}H correlations involving NH protons are related to the chemical shift of the directly bonded ^{15}N atom. For smaller proteins it is relatively rare to find that both the ^{1}H and ^{15}N chemical shifts of two NH groups are degenerate, and hence, these heteronuclear experiments can be used in combination with the conventional homonuclear ones to resolve ambiguities. Recently, this has been applied to the sequential assignment of the helical DNA binding protein Ner where it proved indispensable for resolving ambiguities arising from severe overlap and limited spectral dispersion (Gronenborn et al., 1989b). The power of these experiments lies in overcoming uncertainties in the assignment caused, in particular, by overlap of the NH proton resonances. For proteins larger than about 130 residues, however, it is exactly a region comprising the NH proton resonances, the NH–C$^\alpha$H fingerprint region, where once again not all correlations can be recognized because of severe multiple cross-peak overlap.

In contrast, when 2D NMR is extended into a third dimension, cross-peak overlap is largely removed. Any 3D NMR experiment can be conceived by simply combining two 2D NMR experiments, leaving out the detection period of the first and the preparation period of the second (Griesinger et al., 1987). The first applications to proteins involved homonuclear 3D experiments of the HOHAHA–NOESY type (Oschkinat et al., 1988, 1989; Vuister et al., 1988). While elegant, the applicability of the homonuclear 3D experiment to large proteins is limited as the efficiency of the scalar correlation step is severely reduced with increasing line widths. A more useful set of 3D experiments suggests itself by simply converting the 2D relayed HMQC experiments into corresponding 3D experiments. To date, the only 3D heteronuclear experiments reported for proteins have been the HMQC–NOESY (Fesik & Zuiderweg, 1988) and NOESY–HMQC (Bax et al., 1988; Marion et al., 1989; Zuiderweg & Fesik, 1989) ones. The application of the second experiment to staphylococcal nuclease (Marion et al., 1989) and the anaphylatoxin C5a (Zuiderweg & Fesik, 1989) clearly demonstrated their potential power for spectral simplification as they effectively generate a series of two-dimensional NOESY spectra edited by the chemical shift of the directly bonded ^{15}N atoms.

With respect to sequence-specific assignment of protein ^{1}H NMR spectra, no report has yet been published of the application of 3D NMR to systems where 2D spectroscopic methods have not already proved successful. The 3D HMQC–NOESY or NOESY–HMQC experiment on its own is insufficient for carrying out sequence-specific assignments as there is no simple means of separating out intra- from interresidue effects. Moreover, distinguishing these two effects by reference to a 2D COSY or HOHAHA experiment is difficult in the presence of severe spectral overlap of the NH resonances. Consequently, in those cases that necessitate the use of 3D heteronuclear experiments, a 3D HOHAHA–HMQC or COSY–HMQC experiment is also essential.

In this paper we show for the first time that the combination of three-dimensional ^{1}H–^{15}N HOHAHA–HMQC and NOESY–HMQC experiments, designed to provide the through-bond and through-space connectivities necessary for the sequential assignment procedure, greatly facilitates the sequence-specific assignment of the ^{1}H NMR spectrum of interleukin 1β, a protein of 153 residues. This particular protein is an important component of the immune and inflammatory response systems and, in addition, is directly cytocidal for certain tumor target cells [see Oppenheim et al. (1986) for a review]. Although there have been a large number of functional studies on interleukin 1β, little is known about its detailed mechanism of action. Our own interest is aimed at solving its three-dimensional structure in solution as a first step toward obtaining a better understanding of structure/activity relationships of interleukin 1β.

MATERIALS AND METHODS

Interleukin 1β Preparation and ^{15}N Labeling. Interleukin 1β was purified from *Escherichia coli* harboring the expression vector derived from pPLc24 (Buell et al., 1985) in which interleukin 1β is expressed under control of the bacteriophage λ promotor and the ribosome binding site of the bacteriophage Mu *ner* gene (Wingfield et al., 1986). Uniformly ($\sim$95%) ^{15}N-labeled protein was prepared from bacteria grown in minimal medium with ^{15}NH$_4$Cl as the sole nitrogen source and purified as described previously (Wingfield et al., 1986).

The spectra were recorded on a 2 mM sample dissolved in 150 mM sodium phosphate buffer, 90% H$_2$O/10%D$_2$O, and 0.5 mM sodium azide, pH 7.5, and at a temperature of 27 °C.

Under these conditions at least 120 amide NH peaks can be detected in a regular 2D ^{15}N–^{1}H HMQC experiment.

NMR Spectroscopy. The 3D NOESY–HMQC and HOHAHA–HMQC spectra were recorded on Nicolet NT-500 and Bruker AM600 spectrometers, respectively. Processing of the 3D spectra was carried out on a SUN-4 computer using a simple in-house written routine for the F_2 Fourier transformation (Kay et al., 1989) combined with commercial 2D software (NMR2 from New Methods Research Inc., Syracuse, NY) for the F_1–F_3 2D Fourier transformation.

In addition to the 3D spectra, conventional homonuclear 2D HOHAHA (Braunschweiler & Ernst, 1983; Davis & Bax, 1985) and ^{15}N-edited NOESY (McIntosh et al., 1987a; Senn et al., 1987; Fesik et al., 1988) spectra were also recorded on a Bruker AM600 spectrometer. Water suppression in the ^{15}N-edited NOESY spectrum was achieved with a 1–1 echo read sequence (Sklenar & Bax, 1987b). Water suppression in the HOHAHA spectrum was achieved with a 90° flip back pulse, a fixed recovery delay set to half the mixing time to compensate for rotating-frame Overhauser effects, and the "jump–return" sequence placed after the WALTZ-17$_y$ mixing sequence (Bax et al., 1987). ^{15}N decoupling in F_2 was achieved with a WALTZ-16 decoupling sequence (Shaka et al., 1983) during the acquisition time t_2.

RESULTS AND DISCUSSION

*3D HOHAHA–HMQC and NOESY–HMQC Experiments.* In this section we first describe the two ^{1}H–^{15}N 3D experiments and highlight those practical features that are important for obtaining high-quality spectra.

The general form of the 3D heteronuclear experiment is illustrated along with the HOHAHA–HMQC and NOESY–HMQC pulse sequences in Figure 1. The principles of the NOESY–HMQC experiment have been described in detail (Kay et al., 1989) and are for the most part directly transferable to the HOHAHA–HMQC experiment. The two sequences have in common a DANTE-type off-resonance presaturation of the H_2O signal, a nonselective ^{1}H 90° preparation pulse, a t_1 evolution period, respective mixing period schemes for ^{1}H–^{1}H NOE or HOHAHA transfer, the ^{15}N–^{1}H HMQC filter which incorporates the t_2 evolution time, and finally the detection period during which the signal is recorded as a function of t_3. In both these schemes all ^{1}H and ^{15}N resonances are recorded in F_1 and F_2, respectively, while only the NH region is recorded in F_3. The F_1(^{1}H)–F_3(^{1}H) projection corresponds to the F_1(^{1}H)–F_2(NH) region of a regular ^{1}H–^{1}H NOESY or HOHAHA spectrum and thus ensures that NH–C$^\alpha$H connectivities can be easily observed very close to the water resonance. [In the F_1(NH)–F_2(C$^\alpha$H) region of a 2D-NOESY spectrum, a width of at least 0.7 ppm centered about the water is unobservable due to a large band of t_1 noise.] The F_1(^{1}H)–F_2(^{15}N) projection corresponds to the 2D NOESY–HMQC spectrum (which can only be recorded with ^{1}H in F_2 and ^{15}N in F_1) and the F_2(^{15}N)–F_3(^{1}H) projection to the 2D HMQC spectrum.

The minimal phase cycling for both 3D experiments involves four steps, two for axial peak suppression in F_1 and two for the ^{15}N filter. Using twice the minimum number of scans (eight), we find it is convenient to record each 3D spectrum over a total period of 3–4 days.

The HOHAHA mixing period comprises a 1.5-ms trim pulse along the y axis of the rotating frame, followed immediately by a ^{1}H 90° pulse that returns the magnetization to the z axis. The WALTZ-16 sequence (Shaka et al., 1983) causes isotropic mixing of this magnetization, and the final ^{1}H "read" 90° pulse returns the magnetization to the transverse
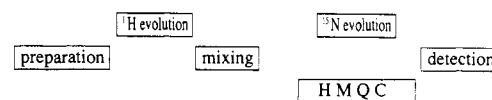
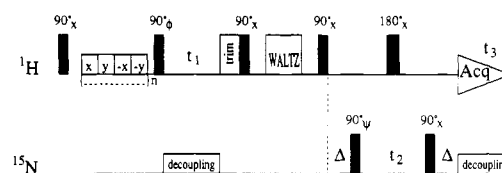**B) 3D NOESY-HMQC Spectroscopy**
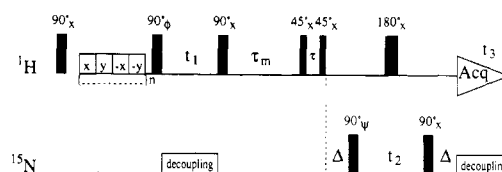
C) 3D HOHAHA-HMQC Spectroscopy

FIGURE 1: (A) Schematic representation of the 3D heteronuclear pulses sequences described in this paper. (B) The 3D HOHAHA–HMQC and (C) 3D NOESY–HMQC pulse sequences. The ^{1}H carrier is positioned in the center of the amide NH region. The phase cycling to obtain pure phase-absorption spectra by the method of States et al. (1982) is given in both cases by $\phi = x,y,-x,-y$, $\psi = 4(x),4(-x)$, and Acq. $= 2(x),4(-x),2(x)$ with data for odd- and even-numbered scans stored separately. For quadrature detection in the F_2 dimension the sequence is repeated with the phase ψ incremented by 90°. No dummy scans are used to achieve a steady state in these experiments because of the significant wastage of time they would entail. They are replaced either by a hard ^{1}H 90°$_x$ pulse (shown in the figure) or by a 20-ms high-power (4W) ^{1}H pulse at the beginning of each t_1 increment. The DANTE presaturation was applied for 1.5 s and makes use of a very weak rf field (10–15 Hz). A 10-ms homospoil pulse was applied in the middle of the NOESY mixing period τ_m to improve H_2O suppression. The NOESY mixing time employed was 100 ms, and the total acquisition times for the NOESY–HMQC experiment were 23.2, 21.8, and 64 ms in t_1, t_2, and t_3, respectively. The duration of the WALTZ-16 mixing sequence was 30.4 ms, and the delays immediately before and after the WALTZ-16 mixing sequence were each set to 8 ms to compensate for rotating-frame NOE effects. Total acquisition times for the HOHAHA–HMQC experiment were 21.4, 20.2, and 66.0 ms in t_1, t_2, and t_3, respectively. For both 3D experiments the ^{15}N–^{1}H coupling evolution and refocusing time Δ was set to 4.5 ms, slightly less than $1/(2J_{NH})$ in order to compensate for T_2 relaxation. ^{15}N decoupling was carried out on a "hard-wired" decoupler unit utilizing GARP (Shaka et al., 1985) phase modulation. The ^{15}N carrier frequency was set in the middle of the ^{15}N spectrum, 120 ppm downfield from liquid ammonia. The total measuring times for the HOHAHA–HMQC and NOESY–HMOC spectra were approximately 2.7 and 3.5 days, respectively.

plane. The incorporation of a fixed delay immediately before and after the WALTZ-16 pulse train is used to remove rotating-frame NOE effects in a manner analogous to that described by Griesinger et al. (1988). These delays additionally allow time to switch the transmitter offset for the mixing sequence to a frequency that maximizes the efficiency of the HOHAHA magnetization transfer between the amide NH and C$^\alpha$H protons ($\sim$1.3 ppm downfield of the H_2O resonance at 6.0 ppm).

One significant difference in the application of these two experiments is the use in the NOESY–HMQC sequence of an off-resonance 1–1 type read pulse (Clore et al., 1983). This is used to help suppress the residual H_2O magnetization present at the end of the mixing time and allows the power of the presaturation pulse train to be minimized. In the case of the HOHAHA–HMQC experiment, mild preirradiation together with the dephasing of the water signal that occurs during the
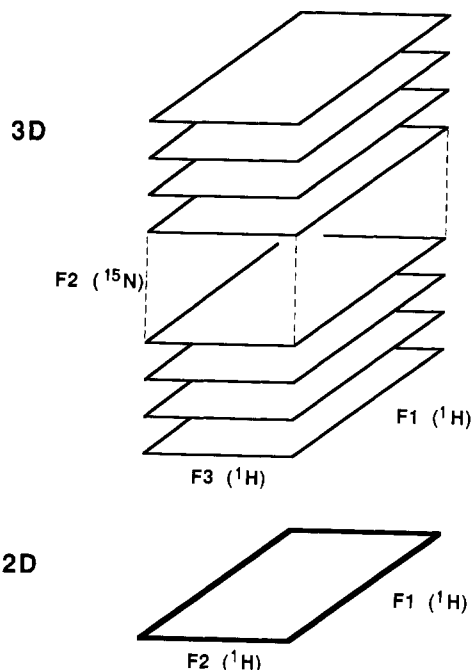
FIGURE 2: Schematic representation of the relationship between the 3D heteronuclear spectra recorded in this paper and conventional homonuclear 2D spectra. The 3D spectrum is viewed as a series of $F_1(^1H)$ slices edited by the chemical shift of the directly bonded ^{15}N atom along the F_2 axis. With 3D spectroscopy it is always important that the digitization be sufficient to resolve the necessary spectral features but not so great that the recording time and data storage requirements become prohibitive. A typical 3D data set is recorded with 128 complex data points in t_1 and 32 complex data points in t_2. Depending on the type of data acquisition used by the spectrometer (i.e., simultaneous or sequential), 256 complex or 512 real data points are collected in t_3. To reduce the required spectral width in F_3 and hence enhance the F_3 digital resolution, the ^1H pulses are applied in the center of the amide NH region of the spectrum, around 3.3 ppm downfield of the solvent H_2O resonance (ca. 8.0 ppm). To shift the carrier and unfold the spectrum in the F_1, an additional linear phase correction of the t_1 time domain data is applied during the processing. The spectra were processed essentially as described by Kay et al. (1989) with a few modifications. The data were first transformed in the F_2 dimension, and the $F_1(^1H)$–$F_3(NH)$ planes, displayed as conventional 2D ^1H–^1H spectra, were then obtained by 2D Fourier transformation. The first-order phase corrections for both the F_1 and the F_2 dimension are given by $360[(4/\pi)\tau_{90°}(^1H) + t_1(0)]/\Delta t_1$ and $360[\tau_{180°}(^1H) + (4/\pi)\tau_{90°}(^{15}N) + t_2(0)]/\Delta t_2$, respectively. A time domain convolution difference-type base-line correction was applied in F_3 (Marion et al., 1989). (For this purpose it is convenient that the H_2O resonance is on the right edge of the spectrum in F_3.) Zero filling was used in all three dimensions to give, for the absorptive part of the spectrum, a matrix of $64 \times 256 \times 512$ data points. The processed 3D spectrum was handled as 64 complete 2D slices plotted onto large pieces of paper (60 cm $\times$ 30 cm). For the purposes of the assignment analysis, sets of four slices from widely separated ^{15}N chemical shifts were plotted in different colors on the same piece of paper. The color coding of slices circumvents any problems of spectral overlap between the four disparate slices. Thus, discarding a few slices toward the edge of the ^{15}N spectral width that contain no signal, the whole of each 3D spectrum could be reduced to a workable total of 13 sheets of paper.

trim pulse is sufficient. (Note that no H_2O recovery occurs during the WALTZ-16 mixing period.)

In recording and presenting the 3D experiments, an effort has been made to retain the characteristics of the corresponding 2D experiments. Thus the spectra obtained can be regarded as a "stretched-out" ^{15}N-edited spectrum with each ^1H–^1H plane representing the identical region covered by the 2D experiment, only containing many fewer cross-peaks (Figure 2). In this way the normal rules for making the sequence-specific assignment of residues can be readily applied.

The only difference with regard to the 3D experiments is that connections between one residue and the next must be made not only between different sets of peaks but between different planes of the spectrum as well. The major advantage, however, is that resolution of overlapping cross-peaks into three-dimensions removes most of the ambiguities present in the 2D spectra. Moreover, the 3D experiments are recorded as a set of 2D ^1H–^1H (t_1, t_3) experiments, with the t_2 delay incremented after the acquisition of each 2D data set. This makes for straightforward programming of the sequence and subsequent data processing.

Application to Interleukin 1β. Interleukin 1β, the focus of the current study, is a protein with 153 amino acids and a molecular mass of ~17.4 kDa. A low-resolution X-ray structure (3 Å) has recently been published and has shown that it is entirely composed of β-sheets connected by loops (Priestle et al., 1988). As a subject for NMR studies, interleukin 1β is at the top end of the molecular weight range for which it appeared possible to obtain sequence-specific assignments by conventional 2D homonuclear techniques. Figure 3A, however, shows that the fingerprint region of the 2D ^{15}N-edited NOESY and ^{15}N-decoupled HOHAHA spectra of this protein is very complex, with many overlapping cross-peaks. The spectrum does not yield easily to the traditional 2D sequential assignment strategy. For example, we encounter limiting temperature (<40 °C) and pH (pH >4.3) conditions suitable for the study of the protein. In addition, the width of individual resonances appears to be rather large when compared to those of some proteins of similar size (e.g., hen egg white lysozyme and flavodoxin). This factor has limited our ability to identify relayed correlations from the NH protons with HOHAHA spectroscopy and hence has hindered spin system identification.

Figure 3B shows two corresponding slices at $\delta(F_2) = 123.7$ (^{15}N) ppm taken from the 3D NOESY–HMQC and 3D HOHAHA–HMQC spectra of a 2 mM sample of uniformly labeled (~95%) [^{15}N]interleukin 1β at pH 7.5 and 27 °C. Alongside each slice of the 3D experiments, the corresponding regions of the corresponding homonuclear 2D ^{15}N-edited NOESY and ^{15}N-decoupled HOHAHA experiments are plotted. Note that the slices from the 3D experiment exhibit very good sensitivity and are essentially devoid of cross-peak overlap. More importantly, the combination of the 3D NOESY–HMQC and HOHAHA–HMQC experiments allows unambiguous identification of the NOEs that originate from a given amide NH and their connection with the $C^\alpha H$ proton of that residue, as indicated by the dashed lines in Figure 3B for four well-resolved cross-peaks arising from the amides of Val-41, Leu-73, Glu-83, and Glu-149. These lines connect the intraresidue $NH(i)$–$C^\alpha H(i)$ HOHAHA cross-peak with the interresidue sequential $NH(i)$–$C^\alpha H(i-1)$ NOESY cross-peak. Knowledge of the through-bond $NH(i)$–$C^\alpha H(i)$ connectivity from the HOHAHA–HMQC experiment eliminates the difficulty of obtaining its location in the 3D NOESY–HMQC spectrum by reference to 2D HOHAHA and HMQC–HOHAHA spectra. This is especially important for the case of β-sheet structure since the intraresidue $C^\alpha H(i)$–$NH(i)$ NOE is often weak or absent. The almost complete absence of overlap in the whole of the 3D spectra of interleukin 1β means that any degeneracy of the ^1H shifts for the amide NH protons is essentially eliminated: in this particular case, virtually no NH groups with degenerate ^1H and ^{15}N chemical shifts are found. In principle, problems of chemical shift degeneracy can potentially be overcome in 2D spectroscopy by varying the experimental conditions of pH and temperature.
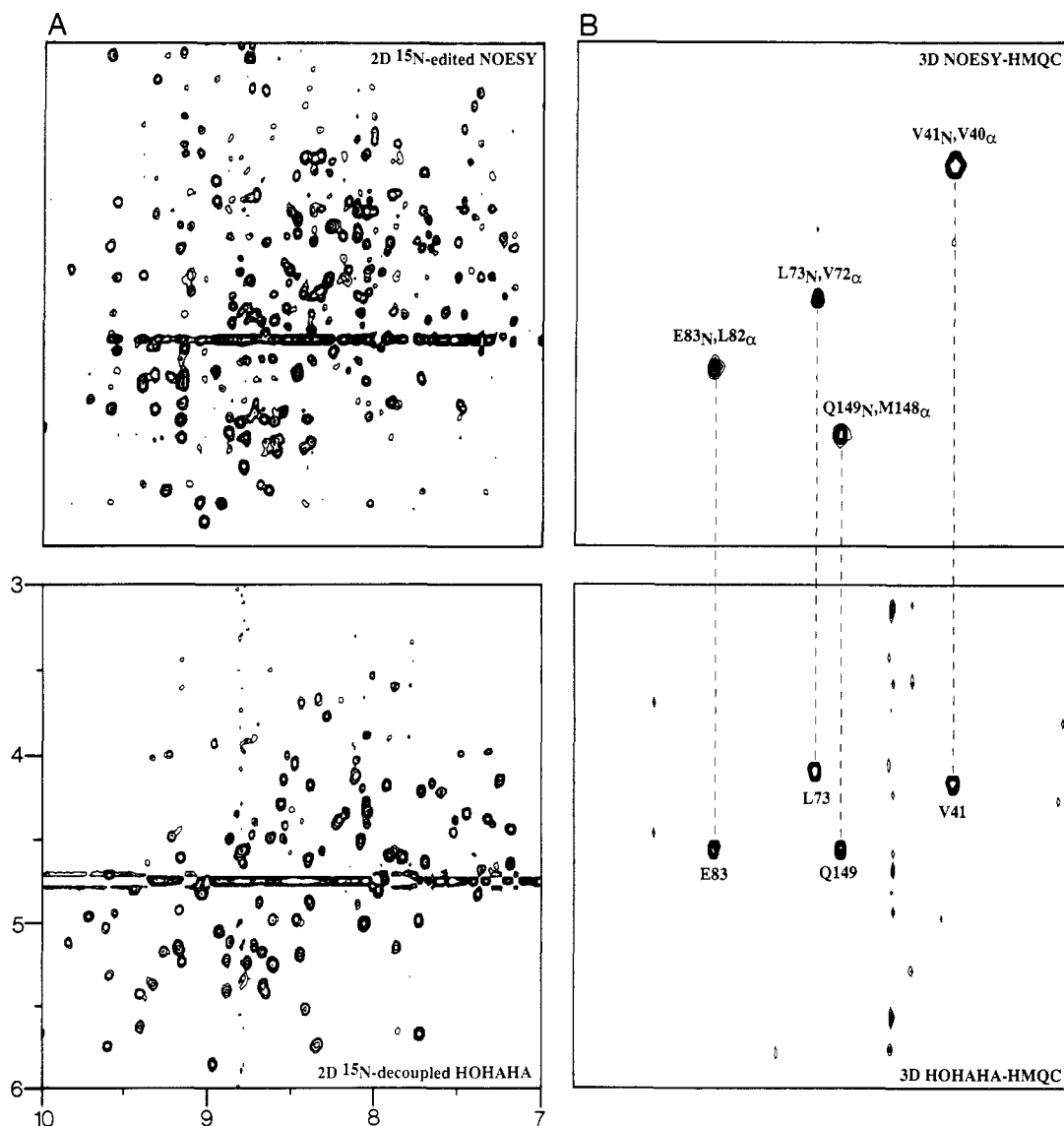
FIGURE 3: (A) Fingerprint regions of the homonuclear ^{15}N-edited 2D NOESY (upper) and ^{15}N-decoupled HOHAHA (lower) spectra of a uniformly ^{15}N-labeled (~95%) sample of 2 mM interleukin 1β recorded at 27 °C and pH 7.5. (B) Corresponding regions of a slice from the 3D heteronuclear NOESY–HMQC (upper) and HOHAHA–HMQC (lower) spectra of the protein under identical conditions. The slice shown corresponds to a ^{15}N chemical shift δ = 123.7 ppm downfield of liquid ammonia.

In the case of large proteins, however, this may simply result in shifting NH degeneracies from one set of spin systems in the 2D spectrum to another set. At the same time different sets of peaks become lost in the ridge created by the residual solvent resonance at the F_1 = 0 frequency. This can be very difficult to keept track of though it may be facilated by computer bookkeeping algorithms (Billeter et al., 1988; Weber & Mueller, 1989). With 3D spectroscopy, NH degeneracies and the corresponding scalar and NOE connectivities can be resolved by inspection of a single 3D spectrum. For example, two spin systems in the spectrum of interleukin 1β which have identical NH and C$^\alpha$H chemical shifts and therefore directly overlapping (NH, C$^\alpha$H) cross-peaks in HOHAHA and COSY spectra are readily resolved in two widely separated planes of the 3D spectra. In particular, the NH(i)–C$^\alpha$H(i) intraresidue cross-peaks of Val-72 and Thr-79 are exactly superimposed in the 2D experiments at δ = 8.75 (NH) and 4.60 (C$^\alpha$H) ppm under the experimental conditions used here. Raising the temperature causes these peaks to disappear into the water ridge line at the F_1 = 0 frequency, and prior to recording the 3D spectrum, they could not be resolved at all in the 2D spectra. The corresponding ^{15}N chemical shifts are 116.8 and

119.7 ppm, respectively, five planes apart in the 3D experiments.

Given the tremendous simplicity of the slices of the 3D spectra, it is a relatively straightforward process to make the sequential assignment by hopping from one pair of HOHAHA/NOESY planes to another pair, connecting them via either C$^\alpha$H(i)–NH($i+1$) or NH(i)–NH($i+1$) NOEs exactly as for the analysis of 2D spectra. This hopping is illustrated for the stretch of residues from Ser-45 to Gln-39 in Figure 4.

Consecutive stretches of sequential NH(i)–NH($i+1$) NOE connectivities in interleukin 1β are readily interpreted from the 3D NOESY–HMQC spectrum, as has been already documented for the anaphylatoxin C5a (Zuiderweg & Fesik, 1989). In a 2D spectrum the NH(i)–NH($i+1$) NOE cross-peaks are located symmetrically about the diagonal in a 2D plane. In the 3D spectrum, on the other hand, they are located symmetrically about the diagonal in 3D space. As the spectra are plotted here as planes perpendicular to the F_2 (^{15}N) coordinate, each NH(i)–NH($i+1$) NOE connection appears in two planes, one peak on each side of the diagnoal. Unambiguous identification of a consecutive stretch of NH(i)–NH-
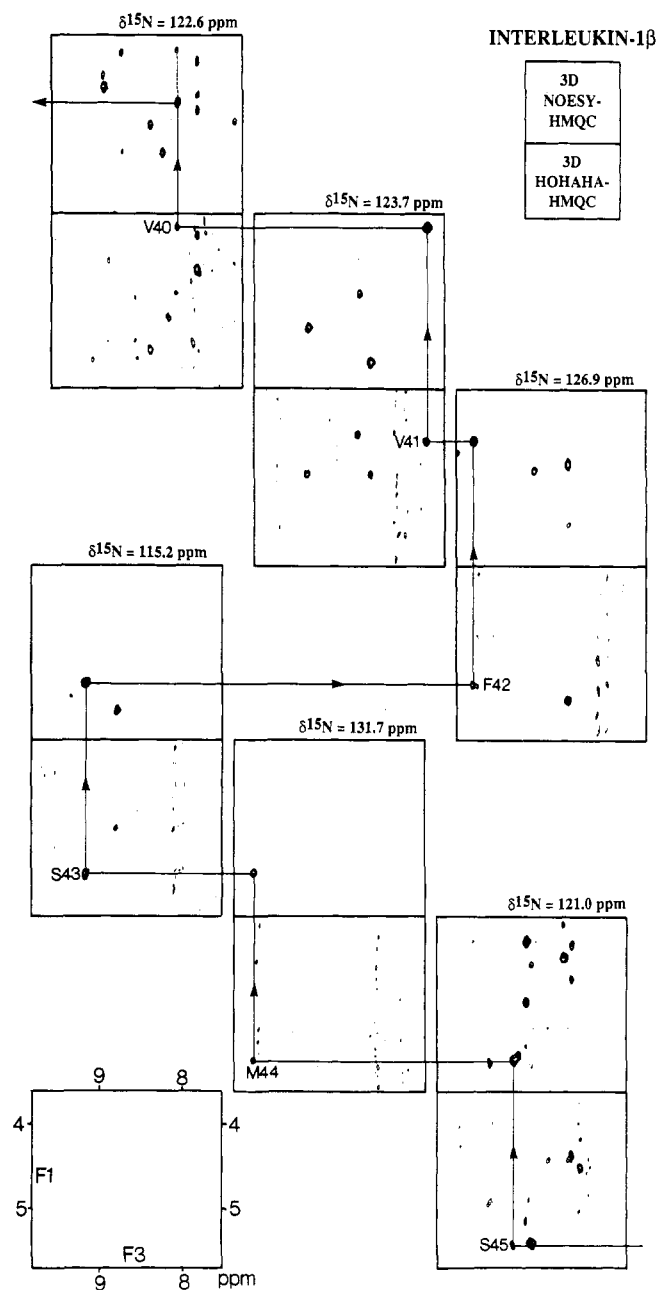
FIGURE 4: Demonstration of the sequential assignment "plane hopping" described in the text for interleukin 1β. Pairs of matching 3D NOESY–HMQC (upper) and HOHAHA–HMQC (lower) planes are shown with the NH(i)–C$^\alpha$H(i)–NH(i+1) connectivities indicated for the stretch of residues Ser-45 to Gln-39. Note, with the exception of Val-41, the absence of intraresidue C$^\alpha$H(i)–NH(i) NOEs in the NOESY planes—typical of an extended strand conformation. Thus, these C$^\alpha$H(i)–NH(i) correlations can only be detected in the HOHAHA planes.

(i+1) connectivities, particularly in a helical protein, depends less on a knowledge of the corresponding C$^\alpha$H chemical shifts, and hence is less dependent on the availability of a 3D HOHAHA–HMQC spectrum, than that for the predominant C$^\alpha$H(i)–NH(i+1) connections found for a β-sheet protein such as interleukin 1β. Clearly, at the interface of stretches of NH(i)–NH(i+1) and C$^\alpha$H(i)–NH(i+1) connected spin systems the 3D HOHAHA–HMQC experiment is invaluable.

Because resonance overlap of both scalar and NOE NH–C$^\alpha$H connectivities is also removed by the 3D ^{15}N–^{1}H heteronuclear experiments, C$^\alpha$H chemical shift determination can be achieved more accurately by 3D than by 2D, so that ambiguities arising from nearly degenerate C$^\alpha$H resonances can

still be overcome. One limitation, however, of the 3D heteronuclear assignment strategy presented in this paper is the presence of absolute C$^\alpha$H chemical shift degeneracy. In general C$^\alpha$H chemical shifts are less sensitive to experimental conditions such as temperature and pH than are amide NH shifts. In the case of 2D spectroscopy the ambiguity arising out of completely degenerate C$^\alpha$H chemical shifts is addressed by the application of additional criteria to the connection of two spin systems, usually by reference to a knowledge of the spin systems types and their agreement with the protein sequence, or by the presence of C$^\beta$H(i)–NH(i+1) NOEs. Unfortunately, for many larger proteins the identification of spin system types or the position of C$^\beta$H chemical shifts is rendered difficult for all but a small number of residues. In the case of interleukin 1β, C$^\beta$H chemical shift identification has proved quite difficult. However, through the unambiguous identification of a small number of assignments from site-directed mutagenesis (Gronenborn et al., 1986; P. C. Driscoll, G. M. Clore, P. T. Wingfield, and A. M. Gronenborn, unpublished data), the identification of a few residues with characteristic side-chain coupling patterns (Gly, Ala, Ser, Thr, Val), and the unequivocal connections obtained from the analysis of the 3D spectra, the assignment of this "large" protein is now tractable.

Additional strategies for completing the assignment include the production of a selected number of specifically labeled samples (e.g., [[^{15}N]Leu]interleukin 1β) to resolve ambiguities still present in the 3D spectra. Thus, for example, there are 15 Leu residues widely dispersed in the sequence of interleukin 1β so that a sample of [^{15}N]Leu-labeled protein would provide 15 umambiguous assignments of residue type.

CONCLUDING REMARKS

We have shown in this paper that 3D heteronuclear NMR spectroscopy can be applied successfully to the assignment of the spectrum of a 153-residue protein. These 3D techniques are comparatively sensitive and can thus be applied to quite dilute samples by NMR standards (less than 2 mM and possibly as little as 0.5 mM). One can record 3D spectra in a reasonable amount of spectrometer time; the 3D HOHAHA–HMQC and NOESY–HMQC experiments together required less than 1 week of measuring time. The overlap of cross-peaks that makes the corresponding 2D spectra impossible to interpret is essentially completely removed. Though identification of spin system types is intrinsically difficult for this size of protein, the 3D spectra can be used as part of an overall assignment strategy, based on selective labeling, site-directed mutagenesis, or conventional NMR spectral analysis. The relative simplicity of the 3D spectra, along with the almost complete absence of overlap in the spectrum, will make them a good starting point for the application of computer-based approaches to automated assignment, even for quite large proteins.

REFERENCES

Bax, A. (1989) *Ann. Rev. Biochem.* (in press).

Bax, A., & Weiss, M. (1987) *J. Magn. Reson. 71*, 571–575.

Bax, A., Griffey, R. H., & Hawkins, B. L. (1983) *J. Am. Chem. Soc. 105*, 7188–7190.

Bax, A., Sklenar, V., Clore, G. M., & Gronenborn, A. M. (1987) *J. Am. Chem. Soc. 109*, 6511–6513.

Bax, A., Clore, G. M., Driscoll, P. C., Gronenborn, A. M., Ikura, M., Kay, L., Marion, D., Sparks, S., & Torchia, D. A. (1988) XIIIth International Conference on Magnetic Resonance in Biological Systems, Madison, WI.

Billeter, M., Basus, V. J., & Kuntz, I. D. (1988) *J. Magn. Reson. 76*, 400–415.

Braunschweiler, L., & Ernst, R. R. (1983) *J. Magn. Reson. 53*, 521–528.

Buel, G., Schulz, M.-F., Selzer, G., Chollet, A., Movva, R., Semon, D., Escanez, S., & Kawashima, E. (1985) *Nucleic Acids Res. 13*, 1923–1938.

Clore, G. M., & Gronenborn, A. M. (1987) *Protein Eng. 1*, 275–288.

Clore, G. M., & Gronenborn, A. M. (1989) *CRC Crit. Rev. Biochem.* (in press).

Clore, G. M., Kimber, B. J., & Gronenborn, A. M. (1983) *J. Magn. Reson. 54*, 170–173.

Davis, D. G., & Bax, A. (1985) *J. Am. Chem. Soc. 107*, 2820–2821.

Ernst, R. R., Bodenhausen, G., & Wokaun, A. (1986) *Principles of Nuclear Magnetic Resonance in One and Two Dimensions*, Clarendon Press, Oxford.

Fesik, S. W., & Zuiderweg, E. R. P. (1988) *J. Magn. Reson. 78*, 588–593.

Fesik, S. W., Gampe, R. T., & Rockway, T. W. (1987) *J. Magn. Reson. 74*, 366–371.

Glushka, J., & Cowburn, D. (1987) *J. Am. Chem. Soc. 109*, 7879–7881.

Griesinger, C., Sørensen, O. W., & Ernst, R. R. (1987) *J. Magn. Reson. 73*, 574–579.

Griesinger, C., Otting, G., Wüthrich, K., & Ernst, R. R. (1988) *J. Am. Chem. Soc. 110*, 7870–7872.

Griffey, R. H., & Redfield, A. G. (1987) *Q. Rev. Biophys. 19*, 51–82.

Gronenborn, A. M., Clore, G. M., Schmeissner, U., & Wingfield, P. T. (1986) *Eur. J. Biochem. 161*, 37–43.

Gronenborn, A. M., Bax, A., Wingfield, P. T., & Clore, G. M. (1989a) *FEBS Lett. 243*, 93–98.

Gronenborn, A. M., Wingfield, P. T., & Clore, G. M. (1989b) *Biochemistry 28*, 5081–5089.

Kay, L. E., Marion, D., & Bax, A. (1989) *J. Magn. Reson.* (in press).

LeMaster, D. M. (1987) *FEBS Lett. 223*, 191–196.

LeMaster, D. M., & Richards, F. M. (1988) *Biochemistry 27*, 142–150.

Marion, D., Kay, L. E., Sparks, S. W., Torchia, D. A., & Bax, A. (1989a) *J. Am. Chem. Soc. 111*, 1515–1517.

Marion, D. A., Ikura, M., & Bax, A. (1989b) *J. Magn. Reson.* (submitted for publication).

Markley, J. L., Westler, W. M., Chan, T. M., Kojiro, C. L., & Ulrich, E. L. (1984) *Fed. Proc., Fed. Am. Soc. Exp. Biol. 43*, 2648–2655.

McIntosh, L. P., Griffey, R. H., Muchmore, D. C., Nielson, C. P., Redfield, A. G., & Dahlquist, F. W. (1987a) *Proc. Natl. Acad. Sci. U.S.A. 84*, 1244–1248.

McIntosh, L. P., Dahlquist, F. W., & Redfield, A. G. (1987b) *J. Biomol. Struct. Dyn. 5*, 21–34.

Mueller, L. (1979) *J. Am. Chem. Soc. 101*, 4481–4484.

Oppenheim, J. J., Kovacs, E. J., Matsushima, K., & Durum, S. K. (1986) *Immunol. Today 7*, 45–56.

Oschkinat, H., Griesinger, C., Kraulis, P. J., Sørensen, O. W., Ernst, R. R., Gronenborn, A. M., & Clore, G. M. (1988) *Nature (London) 332*, 374–377.

Oschkinat, H., Cieslar, C., Gronenborn, A. M., & Clore, G. M. (1989) *J. Magn. Reson. 81*, 212–216.

Priestle, J. P., Schär, H. P., & Grütter, M. G. (1988) *EMBO J. 7*, 339–343.

Rance, M., Wright, P. E., Messerle, B. A., & Field, L. D. (1987) *J. Am. Chem. Soc. 109*, 1591–1592.

Redfield, A. G. (1983) *Chem. Phys. Lett. 96*, 537–540.

Roy, S., Redfield, A. G., Papastavros, M. Z., & Sanchez, V. (1984) *Biochemistry 23*, 4395–4400.

Senn, H., Otting, G., & Wüthrich, K. (1987) *J. Am. Chem. Soc. 109*, 1090–1092.

Shaka, A. J., Keeler, J., Frenkiel, T., & Freeman, R. (1983) *J. Magn. Reson. 52*, 335–338.

Shaka, A. J., Barker, P. B., & Freeman, R. (1985) *J. Magn. Reson. 64*, 547–552.

Shon, H., & Opella, S. J. (1989) *J. Magn. Reson. 82*, 193–197.

Sklenar, V., & Bax, A. (1987a) *J. Magn. Reson. 71*, 379–383.

States, D. J., Haberkorn, R. A., & Reuben, D. J. (1982) *J. Magn. Reson. 48*, 286–292.

Torchia, D. A., Sparks, S. W., & Bax, A. (1988a) *J. Am. Chem. Soc. 110*, 2320–2321.

Torchia, D. A., Sparks, S. W., & Bax, A. (1988b) *Biochemistry 27*, 5135–5141.

Torchia, D. A., Sparks, S. W., & Bax, A. (1989) *Biochemistry* (in press).

Vuister, G. W., Boelens, R., & Kaptein, R. (1988) *J. Magn. Reson. 80*, 176–185.

Weber, P. L., & Mueller, L. (1989) *J. Magn. Reson. 81*, 430–434.

Wilde, J. A., Bolton, P. H., Stolowich, N. J., & Gerlt, J. A. (1986) *J. Magn. Reson. 68*, 168–171.

Wingfield, P. T., Payton, M., Tavernier, J., Barnes, M., Shaw, A., Rose, K., Simona, M. G., Demczuk, S., Williamson, K., & Sayer, J.-M. (1986) *Eur. J. Biochem. 160*, 491–497.

Wüthrich, K. (1986) *NMR of Proteins and Nucleic Acids*, Wiley, New York.

Wüthrich, K. (1989) *Acc. Chem. Res. 22*, 36–44.

Zuiderweg, E. R. P., & Fesik, S. W. (1989) *Biochemistry 28*, 2387–2391.